Enhanced Satellite Attitude Actuation due to Aerodynamic Torque

AUTHORS: Adil Gill, Zayna Khan, and Rayan Syed
University of Illinois at Urbana-Champaign, Urbana, IL 61801, USA

Abstract—

Satellites in low Earth orbit (LEO) are subject to atmospheric drag that generates aerodynamic torques that can both disturb and potentially stabilize attitude dynamics. This paper introduces detumbling simulation that combines a magnetic B-dot controller with aerodynamic torque modeling. Quaternion kinematics is used to propagate the orientation of the vehicle which is a prolate rigid body. Simulations assess the effect of including aerodynamic torque in the existing model, detumbling performance after incorporating altitude-dependent density variations, under different orbital velocities. The results show that using naturally occurring aerodynamic moments can reduce the need for active actuators and provide a low-power stabilization method for CubeSat and tiny satellites. Future work will extend this framework to medium Earth orbit (MEO) environments and explore different control architectures.

I. Introduction

Aerodynamic forces are experienced by satellites in Low Earth Orbit (LEO) due to residual air drag. These forces produce torques that can affect the dynamics of the satellite's attitude, especially for small spacecraft with high ratios of surface area to mass. While commonly treated as disturbances, research suggests that they can be leveraged for passive attitude control when modeled effectively [3]. Recent studies, such as Gargasz *et al.* have shown that in some cases, aerodynamic torque can be utilized as a primary actuation mechanism in addition to a stabilizing force [2]. This paves the path for low-power control techniques that are particularly useful for small satellites and CubeSats. Passive aerodynamic stabilization is particularly attractive for missions that have tight constraints on mass, onboard power, or computational complexity.

Incorporating naturally occurring torques can reduce the need for mechanical actuators, thereby improving system reliability and extending satellite mission lifetimes. It also allows for hybrid control strategies that blend passive and active elements in a more energy-efficient manner.

This study explores the effects of adding aerodynamic torque on detumbling behavior by expanding upon the magnetic B-dot controller design from earlier [6]. The satellite is treated as a rigid, prolate body, and Euler's equations control its motion. Similar missions, like HuskySat-1, have demonstrated the value of integrating passive and magnetic approaches in guidance and control strategies [1]. The aim is to assess the impact of aerodynamic torque on detumbling behavior and determine whether it can be used to increase stability in small satellite systems. The image below shows a satellite in LEO.
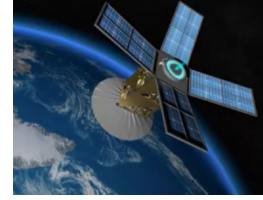

Fig. 1.   A Satellite in Low Earth Orbit (LEO) [3]

We also performed quaternion multiplication and implemented the quaternion kinematics to combine the rotations represented by the quaternions alongside applying the time rate of change of the quaternion.

II. Method

Our method combines the modeling of disturbance torque caused by atmospheric drag in Low Earth Orbit (LEO) with magnetic detumbling using a B-dot controller. The programming language used was Python, the packages used were numpy, matplotlib for plotting and animation in addition to math functions to perform calculation, while the Runge-Kutta 4 method was used for numerical integration. For our dataset, the following initial conditions were used: initial angular velocity $\vec{\omega}_0 = [1.0,\ 0.5,\ -0.2]°/\text{s}$, initial quaternion $q_0 = [1,\ 0,\ 0,\ 0]$, inertia matrix $\mathbf{I} = \text{diag}(0.1,\ 0.15,\ 0.2)\ \text{kg}\cdot\text{m}^2$, and center of pressure offset $\vec{r}_{\text{cp}} = [0.1,\ 0.1,\ 0.1]$ m.

A. Quaternion Kinematics

To track the satellite's orientation in three-dimensional space, we implemented quaternion-based attitude representation. Quaternions avoid singularities and numerical drift common in Euler angle systems. We also performed quaternion multiplication and implemented quaternion kinematics to combine the rotations represented by the quaternions alongside applying the time rate of change of the quaternion. This allowed for accurate propagation of the satellite's attitude over time during simulation.

B. Magnetic Torque and B-dot Control

A magnetic dipole moment m and the Earth's magnetic field B interact to produce magnetic torque, which

is determined by:

$$\mathbf{L}_{\mathrm{mag}} = \mathbf{m} \times \mathbf{B} \qquad [6]$$

For small satellites, a popular passive detumbling technique is the B-dot controller. It uses the cross product of the magnetic field and the satellite's angular velocity to approximate the derivative of the magnetic field with respect to time. The following defines the commanded magnetic moment:

$$\mathbf{m} = -k_B \dot{\mathbf{B}} \approx -k_B (\boldsymbol{\omega} \times \mathbf{B}) \qquad [6]$$

The angular velocity vector of the satellite in the body frame is denoted by $\boldsymbol{\omega}$, whereas k_B represents a positive control gain. A dampening torque that reduces rotational motion is provided by the B-dot algorithm. However, because $\mathbf{m}$ is always perpendicular to B, the control action is always restricted to two axes.

C. Aerodynamic Torque

The atmosphere is sparse but enough in low Earth orbit to cause aerodynamic drag on satellite surfaces. Torque is created when this drag force is deviated from the center of mass. In the inertial frame, the satellite's velocity in relation to the rotating atmosphere is expressed as follows:

$$\mathbf{v}_{\mathrm{rel}} = \mathbf{v}_I + (\boldsymbol{\omega}_{\oplus} \times \mathbf{r}_I) \qquad [6]$$

where $\mathbf{r}_I$ is the satellite's position vector and $\boldsymbol{\omega}_{\oplus}$ is Earth's angular velocity. The body frame is then created from this velocity:

$$\mathbf{v}_{\mathrm{rel},B} = A \begin{bmatrix} \dot{x} + \omega_{\oplus} y \\ \dot{y} - \omega_{\oplus} x \\ \dot{z} \end{bmatrix} \qquad [6]$$

In this case, A represents the attitude rotation matrix from the inertial to body frame, and the velocity components take into consideration planetary rotation and orbital motion.

The following is a model of the aerodynamic force operating on surface i:

$$\mathbf{F}_{\mathrm{aero}}^i = -\frac{1}{2} \rho \, C_D \, \|\mathbf{v}_{\mathrm{rel},B}\| \, \mathbf{v}_{\mathrm{rel},B} \, S_i \, \max(\cos\theta^i, 0) \qquad [6]$$

where:

ρ is atmospheric density (assumed constant in the initial model), C_D is the drag coefficient, S_i is the surface area of panel i, and θ_i is the angle between the velocity vector and the surface normal.

The resulting aerodynamic torque is obtained by summing the cross product of each force and its respective lever arm:

$$\mathbf{L}_{\mathrm{aero}} = \sum_{i=1}^{N} \mathbf{r}^i \times \mathbf{F}_{\mathrm{aero}}^i$$

where $\mathbf{r}^i$ is the vector from the satellite's center of mass to the center of pressure for panel i. Although typically considered a disturbance, this torque may be passively utilized for stabilization if properly modeled.

III. Preliminary Results

In this study, the effects of aerodynamic torque on satellite attitude dynamics were explored by integrating a drag-based disturbance model into a B-dot magnetic detumbling controller. The objective was to see how naturally occurring aerodynamic forces, which are usually regarded as disturbances, impact a satellite's detumbling as it moves through Low Earth Orbit (LEO). We did this by modifying the basic bdot function from class. The simulation was conducted for a prolate satellite body of size 1 m × 1 m × 2 m where the atmospheric drag is present.
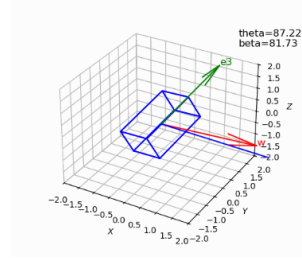

Fig. 2. Prolate Body

Firstly, the effects of aerodynamic torque were observed without taking into consideration the variation in density across LEO and the inclination angle that were responsible for the atmospheric drag. The table below shows the values that were used for the simulation:

TABLE I
Simulation Constants and Parameters

Parameter	Symbol	Value	Unit
Earth grav. parameter	μ_{earth}	3.986×10^{14}	m^3/s^2
Earth radius	R_{E}	6.371×10^6	m
Orbit altitude	h	1.00×10^5	m
Orbit radius	r_{orbit}	6.471×10^6	m
Orbit period	T_{orbit}	5.186×10^3	s
Orbital angular rate	ω_{orbit}	1.211×10^{-3}	rad/s
Earth rotation rate	ω_E	7.292×10^{-5}	rad/s
Inertia tensor (diag. moments)	I	$\mathrm{diag}(0.1, 0.15, 0.2)$	kg·m^2
Drag coefficient	C_d	2.2	—
Ref. area	A	0.01	m^2
Rel. velocity (const.)	v_{rel}	7.5×10^3	m/s
CoP offset	$\mathbf{r}_{cp}$	$[0.1, 0.1, 0.1]$	m
B-dot gain	k_B	5.0×10^4	—

When the satellite is in space, there is no aerodynamic turbulence acting upon the satellite, and hence only the effect of the B-dot controller is present. The figure below demonstrates the satellite stabilization in this instance:
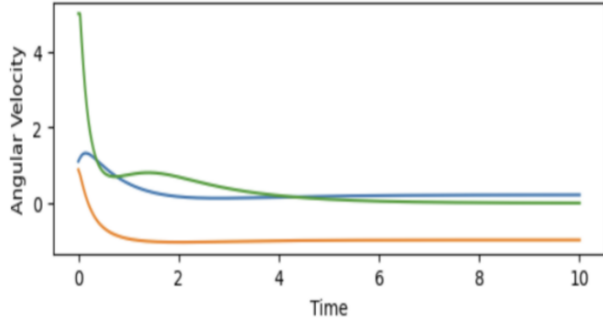
Fig. 3.   Satellite stabilization without aerodynamic torque

However, when the satellite in LEO, its behavior changes drastically due to the aerodynamic drag. As shown in Figure 4, the inclusion of aerodynamic torque resulted in a longer detumbling time compared to simulations using only the B-dot controller.
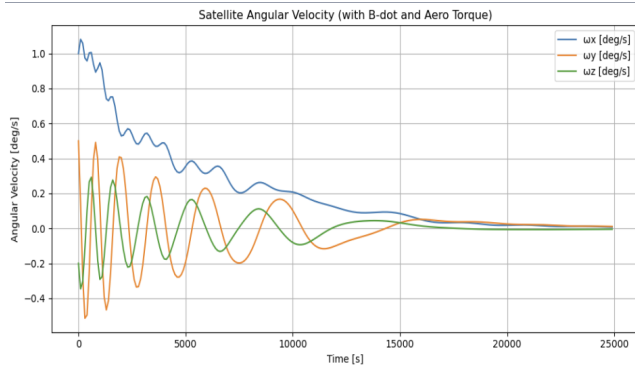

Fig. 4.   Detumbling Time Graph

A.   Density variance with altitude

Following our initial results, we implemented an altitude-dependent atmospheric density model based on our preliminary findings. The model is founded on the standard exponential decay law [7]:

$$\rho(h) = \rho_{\text{ref}} \exp\left(-\frac{h - h_{\text{ref}}}{H}\right)$$

where $\rho_{\text{ref}} = 5.6 \times 10^{-7}\,\text{kg/m}^3$ at $h_{\text{ref}} = 100\,\text{km}$, and the scale height $H = 29.3\,\text{km}$. In light of this model, we now examine how the variation of ρ with altitude in LEO affects satellite behavior. The plot below shows the response at the lowest point of LEO ($h \approx 160$ km):
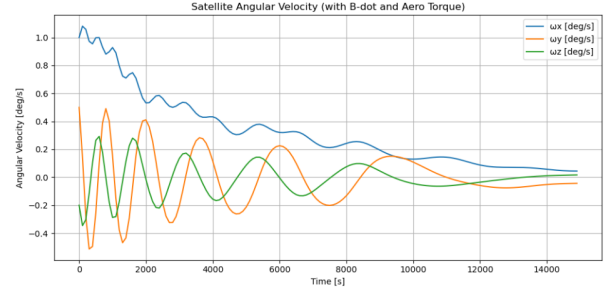

Fig. 5.   Detumbling behavior at the altitude of 160 km

The following table shows the values of density, drag force, and torque:

TABLE II
Aerodynamic Properties at 160 km Altitude

Parameter	Value
Altitude	160 km
Atmospheric Density ρ	1.290×10^{-13} kg/m^3
Drag Force F_{drag}	4.258×10^{-13} N
Torque T_x	-4.258×10^{-14} N·m
Torque T_y	$+4.258 \times 10^{-14}$ N·m
Torque T_z	0.000 N·m

Here, we contrast the result with when the altitude is increased to 2000 km, the highest point of LEO:
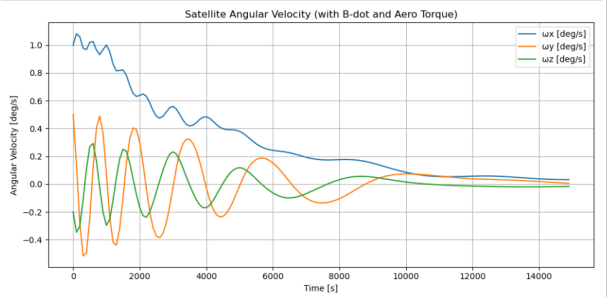

Fig. 6.   Detumbling behavior at the altitude of 2000 km

The values at this altitude are shown below:

TABLE III
Aerodynamic Properties at 2000 km Altitude

Parameter	Value
Altitude	2000 km
Atmospheric Density ρ	6.880×10^{-41} kg/m^3
Drag Force F_{drag}	2.270×10^{-40} N
Torque T_x	-2.270×10^{-41} N·m
Torque T_y	$+2.270 \times 10^{-41}$ N·m
Torque T_z	0.000 N·m

Based on our results, we observe that the density of the atmosphere, the drag force and the aerodynamic torque all vary inversely with the altitude, since going from the

lowest to the highest point of LEO decreased the torque by a factor of 10^{27}, while the magnetic control (B-dot) stays the same in both scenarios. Furthermore, we also notice that the time needed for the satellite to stabilize at lower altitude (high torque) is between 12000 to 14000 seconds. In comparison to this, at higher altitude (low torque), the time for stabilization decreases to around 10000 to 12000 seconds.

B. Effect of angle on Torque

Hereafter we will add the effects of the orientation angle with respect to the Body frame. Angle alignment is significant in producing a physically accurate drag model over a surface, since it shows how aligned the velocity vector is to the normal of the surface. The tables below highlight the difference between τ_{drag}, F_{drag}, and ω at an altitude of 160 km, wherein the former is without any angle implementation, while the latter is when $\theta = 89.616°$:

TABLE IV
Aerodynamic Forces and Dynamics Without $\cos(\theta)$

Quantity	Value
Drag Force $\vec{F}_{\text{drag}}$	$[-1.673 \times 10^{-6},$ $-4.462 \times 10^{-8},$ $1.115 \times 10^{-8}]$ N
Torque $\vec{T}_{\text{aero}}$	$[-2.231 \times 10^{-9},$ $8.366 \times 10^{-8},$ $0.0]$ N $\cdot$ m
Angular Velocity $\vec{\omega}_{\text{new}}$	$[0.01004,$ $0.01999,$ $0.00495]$ rad/s

TABLE V
Aerodynamic Forces and Dynamics With $\cos(\theta) = 0.0067$

Quantity	Value
Drag Force $\vec{F}_{\text{drag}}$	$[-3.750 \times 10^{-5},$ $-1.000 \times 10^{-6},$ $2.500 \times 10^{-7}]$ N
Torque $\vec{T}_{\text{aero}}$	$[0.0,$ $-2.5 \times 10^{-8},$ $-1.0 \times 10^{-7}]$ N $\cdot$ m
Angular Velocity $\vec{\omega}_{\text{new}}$	$[0.01000,$ $0.01999833,$ $0.00498125]$ rad/s

Comparing the two scenarios, the drag force is significantly reduced due to the angle implementation, since the velocity and the surface normal vector are almost perpendicular while without any angle they were perfectly aligned. The influence of torque is also shifted from y axis to z axis due to a change in orientations.

C. Effect of reference area on Torque

Since the aerodynamic torque is proportional to the reference area of the satellite, the area was changed so that the effect could be observed on the satellite. The image below shows the results of that simulation.
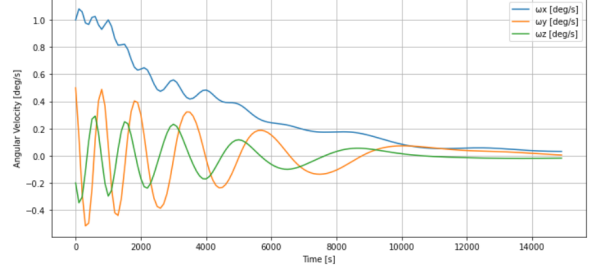

Fig. 7. Effect after increasing the Satellite's reference area

The figure shows the time history of the body-fixed angular velocity components—ω_x (blue), ω_y (orange), and ω_z (green)—following the increase of the reference area (A) to $200\,\text{m}^2$ and the relative velocity (v_{rel}) to $8\,000\,\text{m/s}$. At $t = 0$, $\omega_x \approx 1.05\,\text{deg/s}$, whereas ω_y and ω_z oscillate between roughly $+0.5\,\text{deg/s}$ and $-0.3\,\text{deg/s}$. The enlarged drag torque immediately dissipates rotational energy as the ω_x decays smoothly and steadily, reaching near zero by $t \approx 10\,000\,\text{s}$. Increasing A and v_{rel} increases τ_{drag} by a factor of approximately 2.28×10^4, reducing the detumble time so that all three components collapse to near zero in under 1.5×10^4 s.

IV. Conclusion and Future Works

To determine their effects on aerodynamic torque and detumble time, we changed the panel incidence angle, altitude-dependent density, and reference area in our quaternion-based simulations. We discovered that torque increases proportionally with area, decreases exponentially with altitude (stretched detumbling), and peaks at face-on orientations and disappears at oblique incidence angles. It was observed that the integration of a a high-fidelity aerodynamic torque model with a magnetic B-dot controller can improve attitude stabilization for small satellites in LEO. By using quaternion kinematics alongside an exponential atmospheric density model, we quantified how density falls off by more than 27 orders of magnitude between $160\,\text{km}$ and $2000\,\text{km}$. Additionally, our torque calculations produced accurate moment vectors and explained the underdamped oscillations for ω_y and ω_z when the panel incidence angle ($\cos\theta$) was included.

For future work the current model would be expanded to Medium Earth Orbit (MEO), where drag is lower due to the lower air density. Since aerodynamic torques in MEO are expected to be minimal, this study will help determine whether passive drag-based management is still feasible or active techniques need to be used instead. Designing attitude-control techniques across several orbital regimes will be guided by mapping this transition.

REFERENCES

Bibliography:

T. Reynolds, K. Kaycee, B. Barzgaran, M. Hudoba de Badyn, S. Rice, E. Hansen, A. Adler, B. Acikmese, and M. Mesbahi, "Development of a generic guidance navigation & control system for small satellites: Application to HUSKYSAT-1," *Proc. AIAA SPACE and Astronautics Forum and Exposition*, 2018, doi: 10.2514/6.2018-5403.

M. L. Gargasz, "Optimal spacecraft attitude control using aerodynamic torques," M.S. thesis, Air Force Institute of Technology, 2007. [Online]. Available: https://scholar.afit.edu/etd/2987/

NASA, "Spacecraft aerodynamic torques – space vehicle design criteria /guidance and control/," *NASA Technical Reports Server (NTRS)*, 1971. [Online]. Available: https://ntrs.nasa.gov/citations/19710016459

B. A. 2025 and O. Garvin, "Everything you need to know about CubeSats," Bright Ascension, Dec. 7, 2023. [Online]. Available: https://brightascension.com/everything-you-need-to-know-about-cubesats-2/

"Cranfield University drag sail to stop student satellite becoming space junk," *Institution of Mechanical Engineers (IMechE)*, [Online]. Available: https://www.imeche.org/news/news-article/cranfield-university-drag-sail-to-stop-student-satellite-becoming-space-junk. Accessed: May 13, 2025.

F. L. Markley and J. L. Crassidis, *Fundamentals of Spacecraft Attitude Determination and Control*, Springer, New York, 2014. [Online]. Available: https://doi.org/10.1007/978-1-4939-0802-8

F. Letizia, C. Colombo, and H. G. Lewis, "Analytical model for the propagation of small-debris-object clouds after fragmentations," *Journal of Guidance, Control, and Dynamics*, vol. 38, no. 9, pp. 1741–1756, Sep. 2015. [Online]. Available: https://doi.org/10.2514/1.G000695

R. Syed, A. Gill, Z. Khan, "AE_403_Project_working_density and angle.ipynb," Unpublished Jupyter Notebook, accessed locally, May 14, 2025.

Rayanuzzaman Syed Rayan is a senior pursuing a B.S. degree in Aerospace Engineering at the University of Illinois at Urbana-Champaign.

Zayna Khan Zayna is a senior pursuing a B.S. degree in Aerospace Engineering at the University of Illinois at Urbana-Champaign.

Adil Gill Adil is a senior pursuing a B.S. degree in Aerospace Engineering at the University of Illinois at Urbana-Champaign. He is performing research in the Composites and Additive Manufacturing Lab on composite materials.